

Sensitivity of Source Apportionment of Ambient PM_{2.5}-bound Elements to Input Concentration Data

Tianchu Zhang ¹, Yushan Su ^{2*}, Jerzy Debosz ², Michael Noble ², Anthony Munoz ² and Xiaohong Xu ^{1,*}

Estimation of uncertainty of measured concentrations is described in Zhang et al. [1]. When the concentration is less than or equal to the method detection limit (MDL):

$$Uncertainty = \frac{5}{6} \times MDL \quad (1)$$

When the concentration is greater than the MDL:

$$Uncertainty = \sqrt{(Error\ fraction \times concentration)^2 + (0.5 \times MDL)^2} \quad (2)$$

where error fractions for the 24 PM_{2.5}-bound elements, black carbon and brown carbons are equal to 10% as suggested by other researchers (e.g., Wang et al. [2]; Shin et al. [3]).

Determination of number of factors is described in Zhang et al. [1].

In PMF modeling, the optimal number of PMF-resolved factors is decided by the users. In this study, based on the number of potential sources and the number of measured elements, the optimal number of PMF-resolved factors should be between two and ten. Thus, for each of the five scenarios, PMF model simulations were conducted from two to ten factors to determine an optimal number of factors.

The factor number was determined using three criteria: (1) evaluation of scaled residuals, i.e., IM (maximum individual column mean of scaled residuals), IS (maximum individual column standard deviation of scaled residuals) as well as Q(robust), Q(true), and Q/Q(exp) with factor numbers ranging from two to ten; (2) analysis of the factor matching rates for the bootstrap runs, and (3) interpretability of PMF factor profiles.

Figures S1-S4 show the IM, IS, Q(robust), Q(true), Q/Q(exp) and bootstrap matching rates by the number of factors. IM exhibited the largest decrease when moving from four to five factors (54%), the increment of factors beyond five resulted in less decrease in IM (0.1-17%), which suggests that including more factors than five would not significantly reduce mean scaled residuals of elements involved. The trends of IS, Q(robust), Q(true) and Q/(Qexp) show large drops in values from three to four factors and from four to five factors, and further increase in factor numbers beyond five only leads to a small drop in IS, Q (robust), Q (true), and Q/Q(exp). Furthermore, with the five-factor solution, all factors were mapped in 100% of bootstrap runs, the highest among the nine solutions. Overall, the five-factor solution was the most stable, and explained most of the data variability, and the improvement of the goodness-of-fit of the solutions was marginal beyond the five-factor solution. Therefore, the five-factor solution was selected in Scenario 1.

PMF factor interpretation for Scenario 1

The factor of coal/heavy oil burning was the largest contributor (33%) to total predicted PM_{2.5}-bound elemental concentrations. This factor was characterized by high loadings of S (82%), Se (72%), Br (69%), V (53%) and moderate loadings of Pb (43%), Cr (27%) and K (27%) (Table S2). Pb, S and Se are markers for coal combustion [4, 5, 6], while V is the marker for heavy oil burning [7]. Further, the loadings of Br and Pb in this study are similar to the profiles of Br (50%) and Pb (50%) from coal combustion sources [8] and loadings of Se and V in this study agreed with the profiles of Se (40%) and V (60%) from heavy oil combustions [9]. Although coal-fired power plants were eliminated in Ontario

Citation: Zhang, T.; Su, Y.; Debosz, J.; Noble, M.; Munoz, A.; Xu, X. Sensitivity of Source Apportionment of Ambient PM_{2.5}-bound Elements to Input Concentration Data. *Atmosphere* **2023**, *14*, 1269. <https://doi.org/10.3390/atmos14081269>

Academic Editor: Avelino Eduardo Saez

Received: 1 June 2023

Revised: 21 July 2023

Accepted: 7 August 2023

Published: 10 August 2023



Copyright: © 2023 by the authors. Submitted for possible open access publication under the terms and conditions of the Creative Commons Attribution (CC BY) license (<https://creativecommons.org/licenses/by/4.0/>).

in 2014 [10], coals are still used to generate electricity in the neighboring States, e.g., Michigan, Indiana, and Ohio [11]. Therefore, this factor is likely originated from regional/trans-boundary sources. A PM_{2.5} source apportionment study indicated that the US Midwest, East Coast, and Canada's West were dominant regional sources of sulfate and nitrate in Ontario. That study utilized a trajectory-based simplified quantitative transport bias analysis to identify possible sources of PM_{2.5}-bound sulfate and nitrate factors using PM_{2.5}-bound element data collected from 2005-2010 at five Ontario sites (Windsor, Wallaceburg, Simcoe, Toronto, and Ottawa) [12].

The second-highest contributing factor was vehicular exhaust, contributing an average of 30% of total PM_{2.5}-bound elemental concentrations. This factor is characterized by the high loadings of BrC₁ (93%), BrC₂ (90%), Sn (89%), As (75%), and BC (72%), and moderate loadings of Ba (31%), Cr (27%) and Pb (27%) (Table S2). Diesel vehicle emissions are considered major sources of black carbon [13]. The loadings of BC, Ba and Pb in this study is similar to the profiles of vehicle exhaust from Chen et al. [14], i.e., elemental carbon (65%), Ba (40%), and Pb (40%). High loadings of As in vehicle emissions have been reported in other studies, for example, 65% in Landis et al. [15] and 44% in Balakrishna et al. [16]. Figures S5-S8 show the results of Fpeak rotation that were used to assess the rotational ambiguity in the PMF solutions. The contributions of BC, BrC₁, BrC₂, and Pb to each of the resolved five factors involving a given element changed little among the four selected Fpeak strengths (-1, -0.5, 0.5, 1) when compared with contributions in the base model, suggesting little rotational ambiguity. Further, the number of DISP swaps was zero and the decrease in Q was less than 0.1% (data not shown) at any dQmax levels tested (4, 8, 15, 25), again suggesting there was little rotational ambiguity in the five-factor profiles of PMF solutions. The vehicular exhaust factor had a clear diurnal variability (Figure S9), i.e., peaked in the morning of 6:00-9:00 due to rush hour traffic, and low in the afternoon of 16:00-17:00 due to increased atmospheric mixing height, suggesting this factor is primarily from local sources.

The third-highest contributing factor was metal processing, which was contributing 19% of total PM_{2.5}-bound elemental concentrations. The metal processing factor was dominated by high loadings of Hg (92%), Co (82%), Rb (77%), Ag (73%), Cd (71%), Si (56%), Ni (54%), Cu (44%), K (42%), and Sr (41%), and moderate loadings of Ba (30%) (Table S2). The loadings of Ag, Cd, Co, and Rb are similar to profiles in previous studies, i.e., iron ore and steel industry from Hsu et al. [17] (i.e., Co: 80%) and metal processing from Wang et al. [18] (i.e., 75% of Ag, 50% of Cd, and 30% of Rb). The diurnal variability of metal processing contributions was small (Figure S9), and averaged hour-of-day contributions ranged from 308 ng/m³ at 5:00 to 415 ng/m³ at 8:00, suggesting regional sources of the metal processing factor.

The next-highest contributing factor was crustal dust, contributing 15% of total PM_{2.5}-bound elemental concentrations. The crustal dust factor was characterized by high loadings of Ca (90%), Ti (59%) and Fe (55%) and moderate loadings of Mn (35%), Sr (32%), Ba (31%) and Si (27%) (Table S2). Similar profiles of crustal dust have been reported by Yu et al. [19] that loadings of Ca, Ti, Fe, Si, and Fe are ~80%, 70%, 40%, and 70%, respectively. The crustal dust factor had elevated factor contributions in the morning of 7:00-9:00 (Figure S9), suggesting resuspension of crustal dust by on-road vehicles.

Finally, the lowest contributing factor was vehicle brake and tire wear, contributed 3% of total PM_{2.5}-bound elemental concentrations. The vehicle brake and tire wear factor was characterized by high loadings of Zn (79%) and Mn (58%), and moderate loadings of Fe (26%) (Table S2). Zn is a main tracer of tire wear [20]. Farahani et al. [21] reported loading of 75% of Zn, 5% of Pb and 5% Ti in their profile of tire wear. The loadings of Mn and Fe are similar to the profiles of brake wear from Taghvaei et al. [22] i.e., Mn (30%) and Fe (20%). The diurnal variability of vehicle brake and tire wear was large and in good agreement with other two traffic-related factors, i.e., vehicular exhaust and crustal dust, suggesting the three traffic-related factors are primarily from local sources.

Table S1. Statistics of hourly concentrations for PM_{2.5}, BC and BrCs (µg/m³) and PM_{2.5}-bound elements (ng/m³) during April–October 2021.

a) Scenario 1 (base case) (N= 4362)

Species	Mean	Std Dev	Min	Median	Max	CV (%)	MDL	Missing (%)	<MDL (%)	Flagged (%)	Valid (%)
PM _{2.5}	9.0	5.9	0.5	8	48	152	0.5	1.9	4.1	2.6	91
BC	0.55	0.42	0.0025	0.44	4.8	77	0.005	2.6	0.1	0	97
BrC ₁ *	0.068	0.10	0.001	0.040	2.1	154	NA	2.6	14	0.1	84
BrC ₂ *	0.086	0.082	0.001	0.062	1.6	96	NA	2.6	0.8	0.1	97
Ag	2.6	1.2	2.2	2.2	14	47	4.33	11	73	4.2	11
As	0.3	1.1	0.06	0.1	33	396	0.11	11	72	4.2	13
Ba	2.8	13	0.48	1.0	370	470	0.95	11	40	4.2	45
Br	3.1	2.5	0.09	2.7	49	79	0.18	11	1.3	4.2	83
Ca	84	110	0.45	52	1600	134	0.9	11	0.5	4.2	84
Cd	3.8	1.9	2.9	2.9	17	51	5.75	11	66	4.2	19
Co	0.2	0.1	0.16	0.2	5.7	64	0.32	11	83	4.2	1.1
Cr	0.4	2.7	0.15	0.2	110	757	0.29	11	67	4.2	18
Cu	4.7	10	1.5	3.2	260	209	0.27	11	0	4.2	84
Fe	110	230	0.38	65	7500	209	0.76	11	0.1	4.2	84
Hg	0.6	0.6	0.095	0.5	10	97	0.19	11	24	4.2	60
K	110	260	33	83	7000	229	2.37	11	0	4.2	84
Mn	4.3	8.8	0.14	1.8	150	207	0.28	11	3.6	4.2	81
Ni	0.5	1.6	0.12	0.3	41	311	0.23	11	35	4.2	49
Pb	3.8	7.9	0.25	3.0	340	207	0.22	11	0	4.2	84
Rb	0.2	0.1	0.17	0.2	2.9	63	0.34	11	70	4.2	14
S	580	500	8.1	440	4100	87	6	11	0	4.2	84
Se	0.6	1.1	0.07	0.4	20	167	0.14	11	18	4.2	66
Si	400	210	47	360	3300	52	20	11	0	4.2	84
Sn	3.9	4.2	3.7	3.7	140	105	7.46	11	84	4.2	0.4
Sr	1.5	6.6	0.23	0.9	180	429	0.45	11	7.8	4.2	77
Ti	3.9	4.0	0.19	2.9	55	101	0.38	11	1.5	4.2	83

V	0.5	1.1	0.15	0.2	31	230	0.29	11	55	4.2	29
Zn	24	52	0.12	10	840	216	0.23	11	0.3	4.2	84

Note: Missing (%) + <MDL (%) + Flagged (%) + Valid (%) = 100%.

* BrC₁ and BrC₂ concentrations were calculated.

b) Scenario 3 (N=72)

Species	Mean	Std Dev	Min	Median	Max	CV (%)	<MDL (%)	Valid (%)
PM _{2.5}	19	12	2	17	47	158	0	100
BC	1.0	0.59	0.25	0.83	2.6	58.5	0	100
BrC ₁ *	0.17	0.15	0.003	0.12	0.57	88.9	7	93
BrC ₂ *	0.17	0.12	0.001	0.12	0.44	73.6	1	99
Ag	2.8	1.6	2.2	2.2	10	58.5	65	15
As	0.67	1.1	0.055	0.055	4.5	165	51	29
Ba	55	83	0.47	17	370	151	6	75
Br	4	2.3	1.2	3.3	12	57.5	0	81
Ca	64	52	15	52	260	80.1	0	81
Cd	4.7	3	2.9	2.9	17	63	50	31
Co	0.17	0.034	0.16	0.16	0.42	20.7	79	1
Cr	1	1.8	0.15	0.15	9.7	179	39	42
Cu	42	58	3.2	15	260	140	0	81
Fe	120	150	19	65	820	131	0	81
Hg	0.55	0.61	0.095	0.43	3.5	112	33	47
K	1200	1600	83	450	7000	136	0	81
Mn	6.5	10	0.32	2.9	57	160	0	81
Ni	0.34	0.44	0.12	0.27	2.9	129	39	42
Pb	7.4	5.9	2.2	4.8	29	79.5	0	81
Rb	0.46	0.6	0.17	0.17	2.9	131	47	33
S	680	600	100	440	2900	89.1	0	81
Se	0.45	0.42	0.07	0.36	1.9	93.1	22	58
Si	400	140	160	360	840	35.8	0	81
Sn	17	30	3.7	3.7	140	180	58	22
Sr	29	42	0.87	9.4	180	146	0	81

Ti	9.4	10	1.2	4.4	49	108	0	81
V	0.41	0.91	0.15	0.15	5.7	224	68	13
Zn	28	46	3.4	12	320	164	0	81

Note: Missing (%) + <MDL (%) + Flagged (%) + Valid (%) = 100%

* BrC₁ and BrC₂ concentrations were calculated.

c) Scenario 4 (N=24)

Species	Mean	Std Dev	Min	Median	Max	CV (%)	<MDL (%)	Valid (%)
PM _{2.5}	23	9.8	12	19	43	236	0	100
BC	1.4	0.86	0.26	1.0	3.1	61.1	0	100
BrC ₁ *	0.42	0.64	0.010	0.099	2.1	152	0	100
BrC ₂ *	0.30	0.32	0.033	0.14	1.0	108	0	100
Ag	3.3	2.3	2.2	2.2	11	70.2	71	25
As	1.7	2.9	0.055	0.055	11	175	54	42
Ba	7.9	11	0.47	3.3	41	141	8	88
Br	8.3	10	1.5	4	42	126	0	96
Ca	270	160	24	240	560	57.5	0	96
Cd	3.8	1.7	2.9	2.9	7.3	43.4	71	25
Co	0.66	1.3	0.16	0.16	5.7	199	71	25
Cr	8	25	0.14	0.14	110	308	50	46
Cu	21	30	2.7	6.5	120	142	0	96
Fe	1200	2200	35	370	7500	174	0	96
Hg	1.3	2.4	0.095	0.45	10	184	29	67
K	260	200	97	170	850	78	0	96
Mn	31	36	1.8	16	150	118	0	96
Ni	4.3	8.5	0.12	0.31	26	199	38	58
Pb	12	20	1.3	5.7	96	160	0	96
Rb	0.31	0.19	0.17	0.17	0.95	63.2	54	42
S	560	130	330	520	880	23.7	0	96
Se	0.57	0.46	0.07	0.37	1.7	81.7	4	92
Si	640	200	280	610	1000	31.4	0	96

Sn	3.7	<0.1	3.7	3.7	3.7	<0.1	96	0
Sr	3.5	4.1	0.79	1.9	17	117	0	96
Ti	8.7	4.1	1.9	8.1	20	46.6	0	96
V	0.34	0.51	0.15	0.15	2.5	150	67	29
Zn	63	66	6	36	240	106	0	96

Note: Missing (%) + <MDL (%) + Flagged (%) + Valid (%) = 100%

* BrC₁ and BrC₂ concentrations were calculated.

d) Scenario 5 (N= 4266)

Species	Mean	Std Dev	Min	Median	Max	CV (%)	<MDL (%)	Valid (%)
PM _{2.5}	8.8	5.5	0.5	8	48	159	4	91
BC	0.53	0.41	0.0025	0.44	4.8	76.2	0	91
BrC ₁ *	0.064	0.087	0.001	0.040	1.4	137	14	86
BrC ₂ *	0.083	0.075	0.001	0.062	1.6	90.9	0.8	99
Ag	2.6	1.2	2.2	2.2	14	45.9	73	11
As	0.25	1	0.055	0.055	33	409	72	12
Ba	1.9	3.6	0.48	1	130	192	41	44
Br	3.1	2.3	0.09	2.7	49	75.7	1.3	83
Ca	83	110	0.45	52	1600	135	0.5	84
Cd	3.8	1.9	2.9	2.9	17	50.4	66	18
Co	0.16	0.027	0.16	0.16	0.69	16.8	83	0.9
Cr	0.3	2	0.15	0.15	110	646	67	17
Cu	3.9	3.2	1.5	3.2	83	80.8	0.0	84
Fe	100	150	0.38	65	3700	143	0.1	84
Hg	0.6	0.56	0.095	0.46	6.3	93.1	24	60
K	94	51	33	83	960	55	0	84
Mn	4.1	8.2	0.14	1.8	110	200	3.7	81
Ni	0.49	1.4	0.12	0.27	41	295	35	49
Pb	3.7	7.8	0.25	3	340	209	0	84
Rb	0.21	0.11	0.17	0.17	1.1	51.8	70	14
S	580	500	8.1	440	4100	86.9	0	84

Se	0.64	1.1	0.07	0.36	20	168	18	66
Si	400	210	47	360	3300	52.5	0	84
Sn	3.7	<0.1	3.7	3.7	3.7	<0.1	84	0.0
Sr	1.1	1.6	0.23	0.87	73	147	8.0	76
Ti	3.8	3.7	0.19	2.9	55	96.8	1.5	83
V	0.5	1.1	0.15	0.15	31	230	55	29
Zn	24	52	0.12	10	840	218	0.3	84

Note: Missing (%) + <MDL (%) + Flagged (%) + Valid (%) =100%

* BrC₁ and BrC₂ concentrations were calculated.

Table S2. Factor profiles (% of species mass concentrations being assigned to that factor) for black carbon (BC) and brown carbons (BrC₁ and BrC₂), and PM_{2.5}-bound elements in Windsor during April-October 2021 (Scenario 1). Bold values are percentages ≥40%.

Species	Coal/heavy oil burning	Vehicular exhaust	Metal processing	Crustal dust	Vehicle brake and tire wear
BC	15	79	0	6	0
BrC ₁	0	78	20	0	2
BrC ₂	0	90	3	5	1
Ag	21	6	68	5	0
As	23	65	9	0	2
Ba	5	36	29	28	1
Br	67	14	14	5	0
Ca	0	0	11	87	2
Cd	21	9	67	2	1
Co	18	10	67	3	1
Cr	20	23	33	17	6
Cu	14	21	41	14	10
Fe	8	8	8	53	23
Hg	9	0	83	2	5
K	26	18	41	15	0
Mn	7	4	1	33	55
Ni	19	9	57	14	1
Pb	40	31	23	4	1
Rb	17	9	66	8	0
S	82	0	14	2	2
Se	70	4	22	0	4
Si	17	1	54	28	0
Sn	23	16	60	1	0

Sr	16	11	42	31	0
Ti	17	7	19	58	0
V	42	3	43	11	1
Zn	14	6	0	4	76

Table S3. Factor profiles (% of species mass concentrations being assigned to that factor) for black carbon (BC) and brown carbons (BrC₁ and BrC₂), and PM_{2.5}-bound elements in Windsor during the 1st episodic event on July 3-5, 2021 (Scenario 3). Bold values are percentages $\geq 40\%$.

Species	Fireworks	Vehicular exhaust	Coal burning and metal processing	Crustal dust and tire and brake wear
BC	7	50	38	5
BrC ₁	6	75	15	4
BrC ₂	5	65	22	7
Ag	0	22	63	15
As	0	100	0	0
Ba	74	18	0	7
Br	17	30	43	10
Ca	0	13	36	51
Cd	13	30	50	8
Co	7	20	65	8
Cr	80	9	0	11
Cu	69	18	3	9
Fe	5	14	16	65
Hg	0	10	69	21
K	69	19	3	9
Mn	26	12	3	60
Ni	6	22	51	21
Pb	28	32	28	12
Rb	66	0	31	2
S	56	1	35	8
Se	29	0	43	28
Si	8	18	59	14
Sn	94	0	6	0
Sr	75	15	1	8
Ti	52	21	14	14
V	30	10	45	15
Zn	21	18	14	48

Table S4. List of firework events in Michigan in July 2021 (Data sources: Oilver, [23]; Mlive, [24]).

Date	Start Time	Location
------	------------	----------

July 2 and 3	10:00 PM	20900 Oakwood Blvd. Dearborn, Michigan
July 2, 3, and 4	10:12 PM	301 Washington Ave. Bay City, Michigan
July 3	10:00 PM	32481 West Jefferson Ave, Brownstown Charter Township, Michigan
July 3	10:00 PM	600 West Main Street, Manchester, Michigan
July 4	At dusk	9318 Main Street, Whitmore Lake, Michigan
July 4	At dusk	6598 Brush Street, North Branch, Michigan

Table S5. Factor profiles (% of species mass concentrations being assigned to that factor) for black carbon (BC) and brown carbons (BrC₁ and BrC₂), and PM_{2.5}-bound elements in Windsor during the 2nd episodic event on July 20, 2021 (Scenario 4). Bold values are percentages $\geq 40\%$.

Species	Mineral dust	Coal burning and metal processing	Vehicular exhaust	Crustal dust	Heavy oil burning and metal processing
BC	33	22	18	19	7
BrC ₁	26	5	62	0	7
BrC ₂	34	13	47	6	0
Ag	10	67	19	4	1
As	5	2	56	0	37
Ba	71	7	0	19	3
Br	17	32	46	3	3
Ca	11	18	8	64	0
Cd	12	63	13	4	9
Co	0	17	80	3	0
Cr	2	3	34	7	54
Cu	17	10	34	5	33
Fe	6	1	16	16	61
Hg	6	23	2	0	69
K	46	32	8	10	4
Mn	62	0	10	16	12
Ni	0	0	12	6	82
Pb	19	20	16	19	25
Rb	21	51	17	5	5
S	22	54	11	10	3
Se	27	31	16	10	17
Si	13	44	13	23	7
Sn	17	58	9	12	3

Sr	59	11	1	27	2
Ti	31	29	10	26	5
V	6	16	0	33	45
Zn	10	14	52	23	1

Table S6. Factor profiles (% of species mass concentrations being assigned to that factor) for black carbon (BC) and brown carbons (BrC₁ and BrC₂), and PM_{2.5}-bound elements in Windsor excluding the two episodic events (Scenario 5). Bold values are percentages $\geq 40\%$.

Species	Coal/heavy oil burnings	Vehicular exhaust	Metal processing	Crustal dust	Vehicle tire and brake wear
BC	16	80	0	4	0
BrC ₁	0	74	24	0	3
BrC ₂	0	91	3	4	1
Ag	21	6	68	5	0
As	24	63	11	0	2
Ba	6	35	30	27	2
Br	68	13	14	5	0
Ca	6	1	10	82	2
Cd	20	9	68	2	1
Co	19	9	68	4	0
Cr	21	20	36	18	5
Cu	15	20	41	13	10
Fe	11	9	7	50	23
Hg	9	0	83	3	5
K	27	17	41	14	0
Mn	9	4	1	31	55
Ni	20	11	56	13	1
Pb	41	30	23	4	1
Rb	15	6	70	9	0
S	82	0	14	2	2
Se	70	5	21	0	3
Si	19	0	54	27	0
Sn	21	9	66	3	0
Sr	18	10	42	30	0
Ti	20	7	18	55	0
V	41	5	42	11	1
Zn	14	5	0	4	77

Table S7. Vehicle exhaust factor profiles (% of species mass concentrations being assigned to that factor) in each of the five scenarios. Bold values are percentages $\geq 40\%$.

Species	S1	S2	S3	S4	S5
BC	79	87	50	18	80
BrC ₁	78		75	62	74
BrC ₂	90		65	47	91
Ag	6	7	22	19	6
As	65	90	100	56	63
Ba	36	58	18	0	35
Br	14	15	30	46	13
Ca	0	0	13	8	1
Cd	9	12	30	13	9
Co	10	12	20	80	9
Cr	23	31	9	34	20
Cu	21	32	18	34	20
Fe	8	14	14	16	9
Hg	0	0	10	2	0
K	18	21	19	8	17
Mn	4	7	12	10	4
Ni	9	15	22	12	11
Pb	31	47	32	16	30
Rb	9	9	0	17	6
S	0	0	1	11	0
Se	4	5	0	16	5
Si	1	0	18	13	0
Sn	16	18	0	9	9
Sr	11	16	15	1	10
Ti	7	10	21	10	7
V	3	4	10	0	5
Zn	6	7	18	52	5

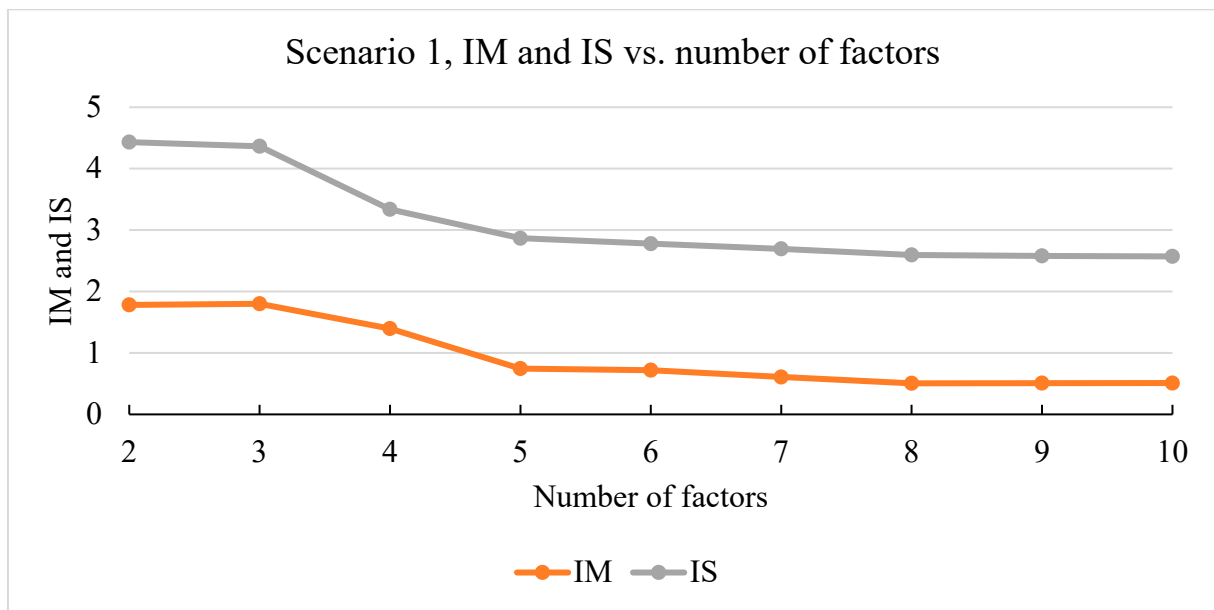


Figure S1. IM and IS vs. number of factors in Scenario 1.

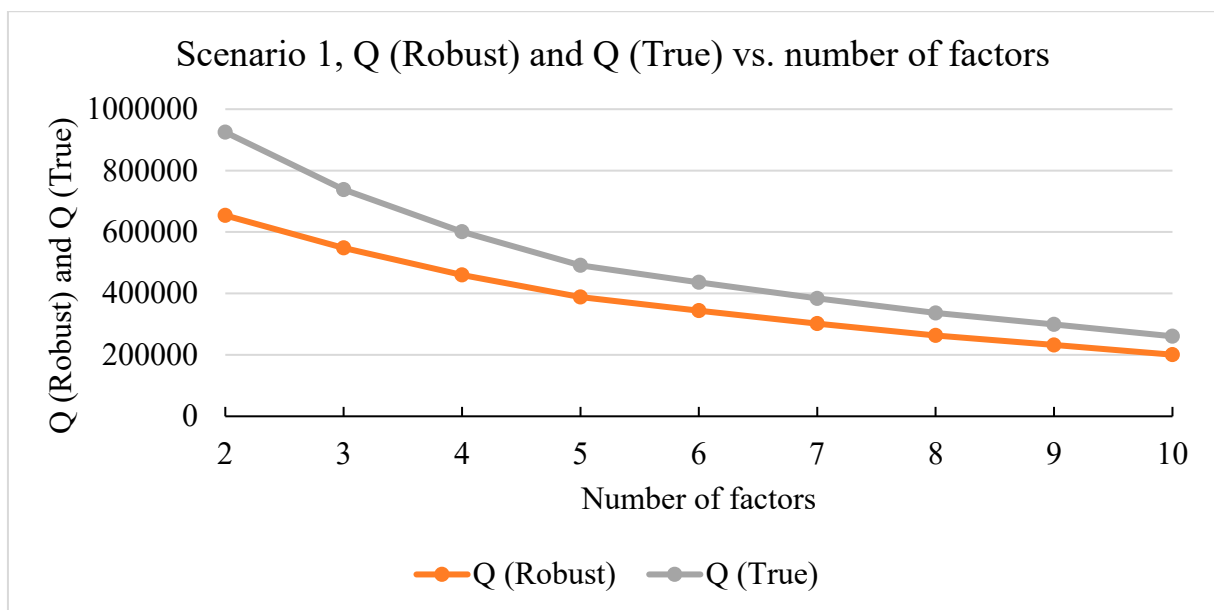


Figure S2. Q (Robust) and Q (True) vs. number of factors in Scenario 1.

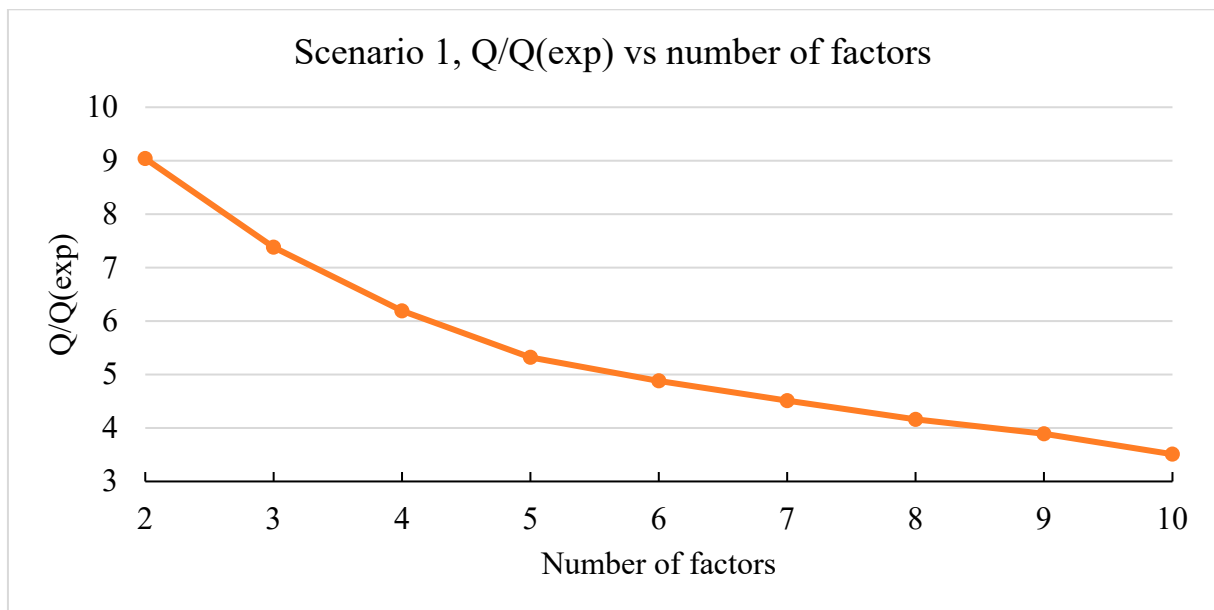


Figure S3. Q/Qexp vs. number of factors in Scenario 1.

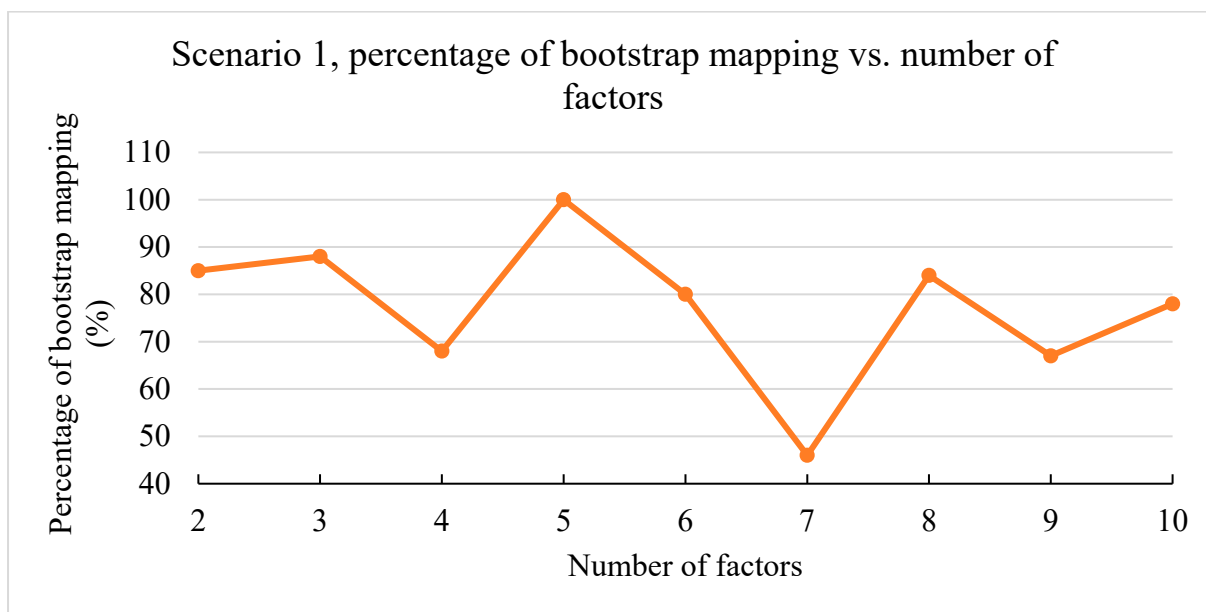
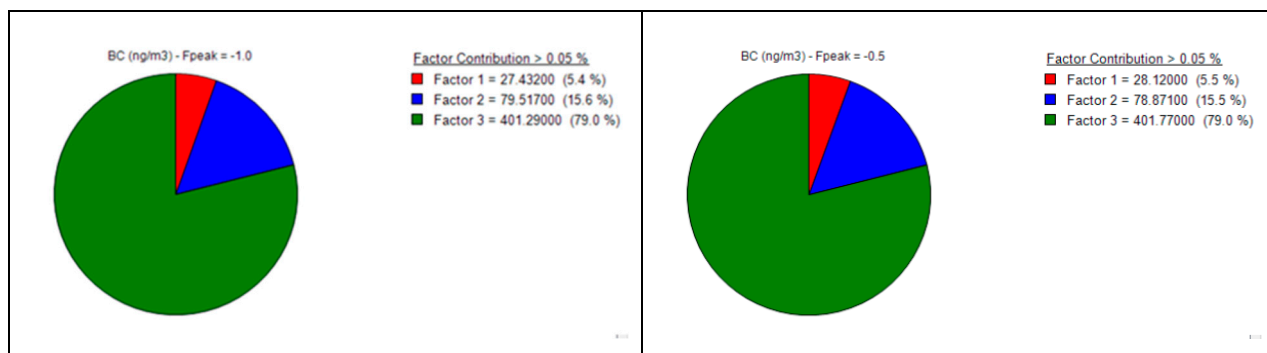


Figure S4. The percentage of bootstrap matching vs. number of factors in Scenario 1.



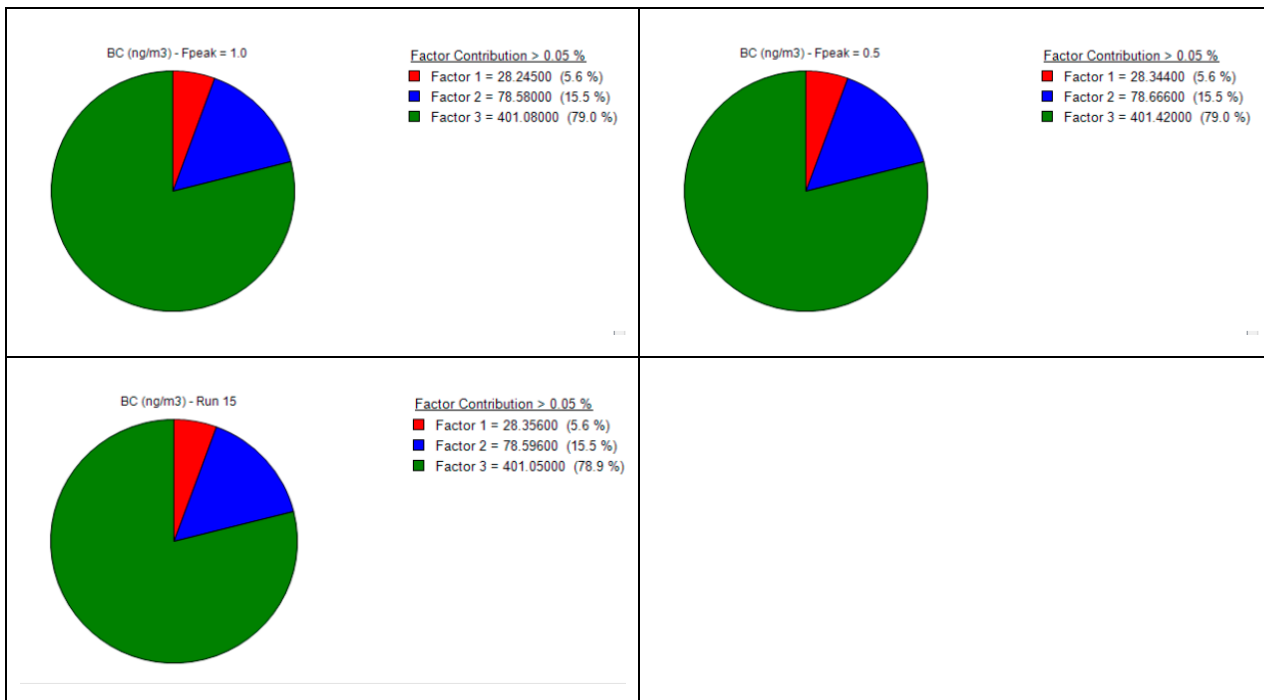


Figure S5. Factor contributions (ng/m³ and %) of BC to individual PMF resolved sources (factors contribution >0.05% is shown) at Fpeak strength of -1, -0.5, 0.5 and 1 in the base model (Run 15) of Scenario 1. Factor 1: Crustal dust, Factor 2: Coal/heavy oil burning, Factor 3: vehicular exhaust.

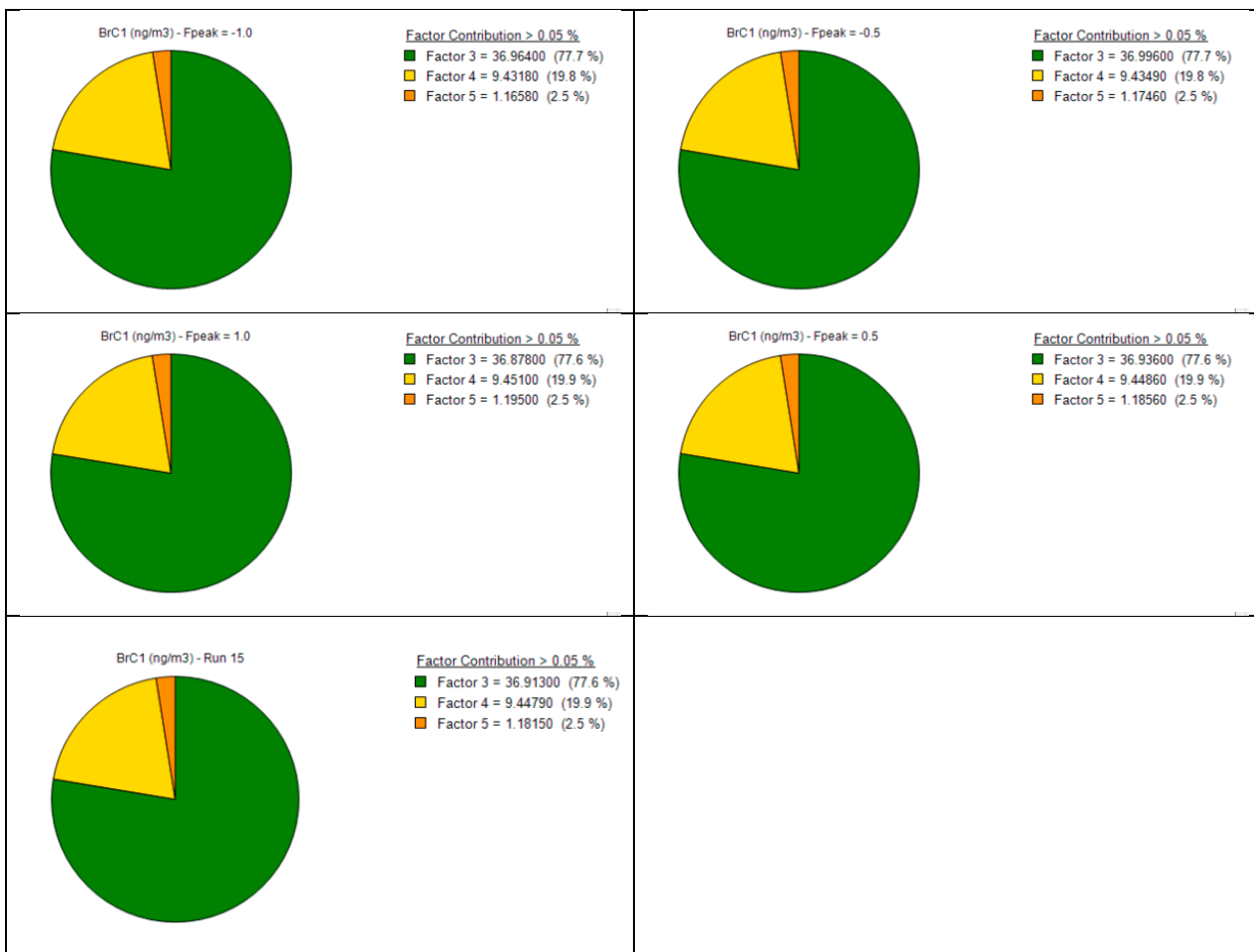


Figure S6. Factor contributions (ng/m³ and %) of BrC₁ to individual PMF resolved sources (factors contribution >0.05% is shown) at Fpeak strength of -1, -0.5, 0.5 and 1 in the base model (Run 15) of Scenario 1. Factor 3: vehicular exhaust, Factor 4: Metal processing, Factor 5: Vehicle tire and brake wear.

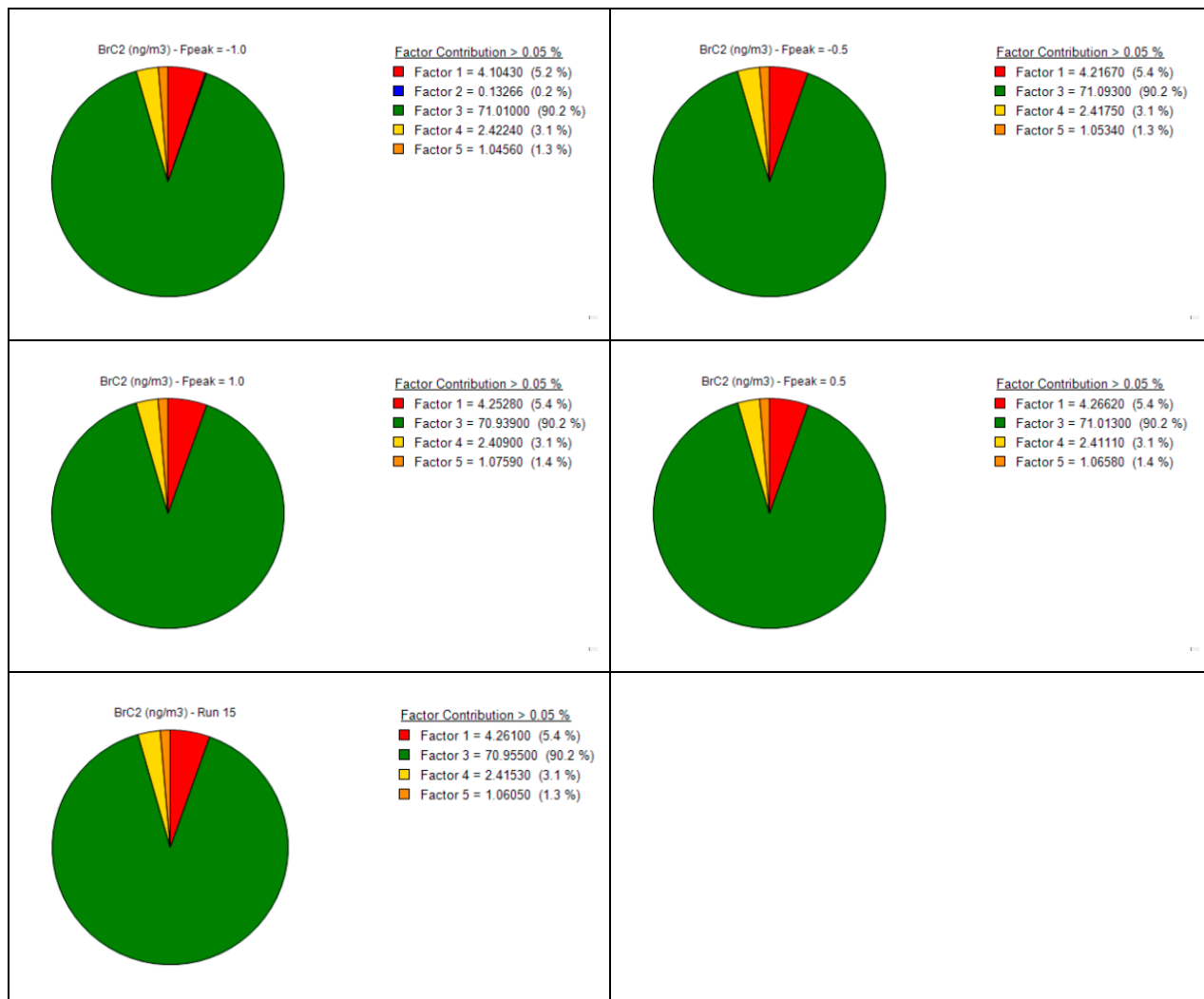
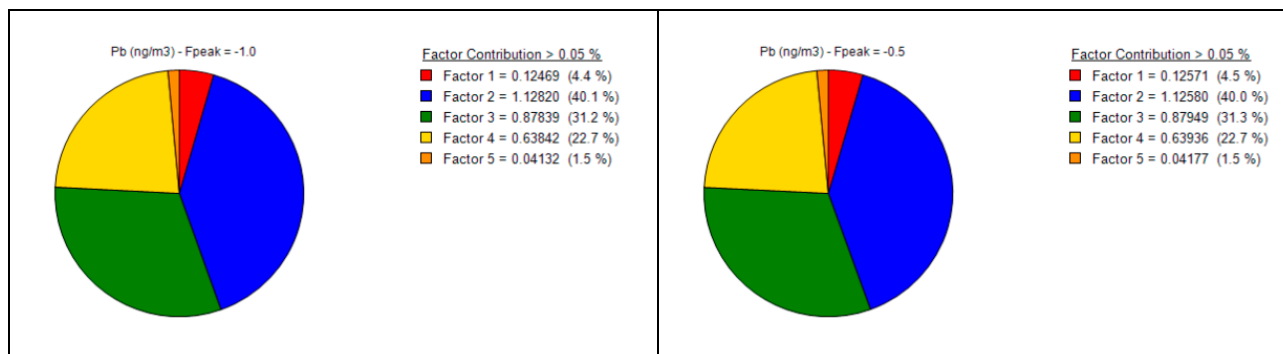


Figure S7. Factor contributions (ng/m³ and %) of BrC₂ to individual PMF resolved sources (factors contribution >0.05% is shown) at Fpeak strength of -1, -0.5, 0.5 and 1 in the base model (Run 15) of Scenario 1. Factor 1: Crustal dust, Factor 2: Coal/heavy oil burning, Factor 3: vehicular exhaust, Factor 4: Metal processing, Factor 5: Vehicle tire and brake wear.



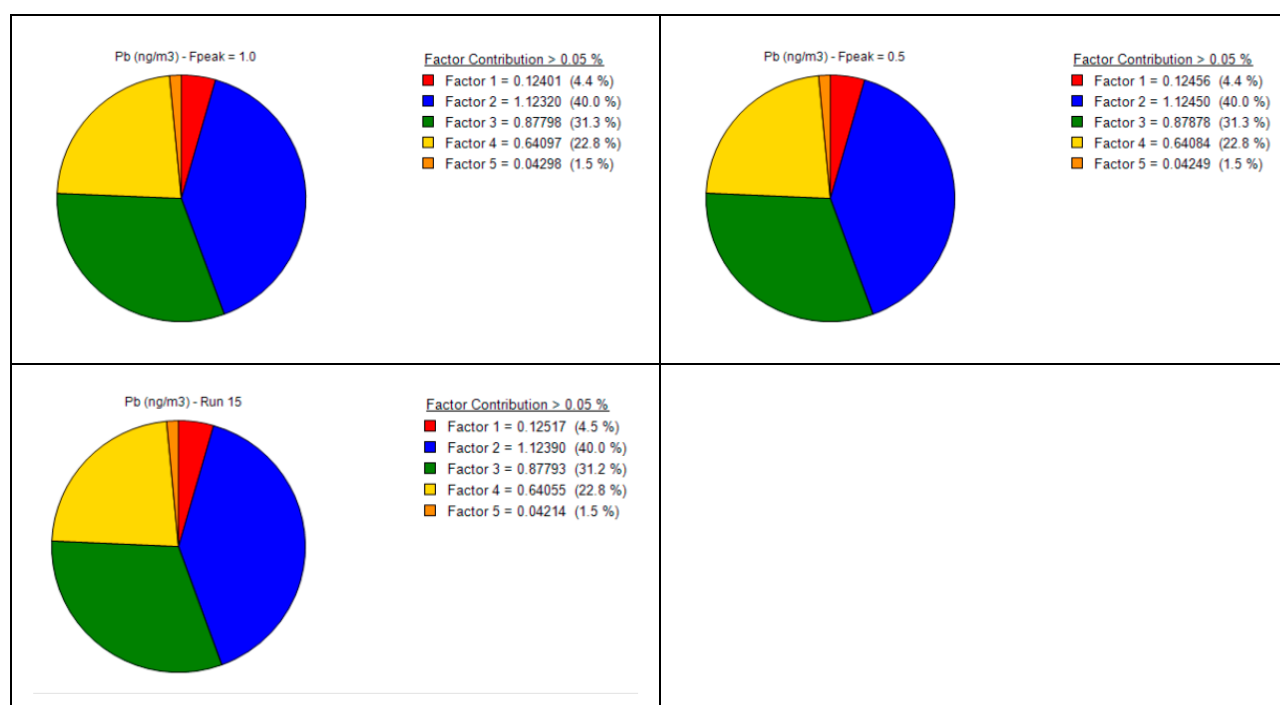


Figure S8. Factor contributions (ng/m³ and %) of Pb to individual PMF resolved sources (factors contribution >0.05% is shown) at Fpeak strength of -1, -0.5, 0.5 and 1 in the base model (Run 15) of Scenario 1. Factor 1: Crustal dust, Factor 2: Coal/heavy oil burning, Factor 3: vehicular exhaust, Factor 4: Metal processing, Factor 5: Vehicle tire and brake wear.

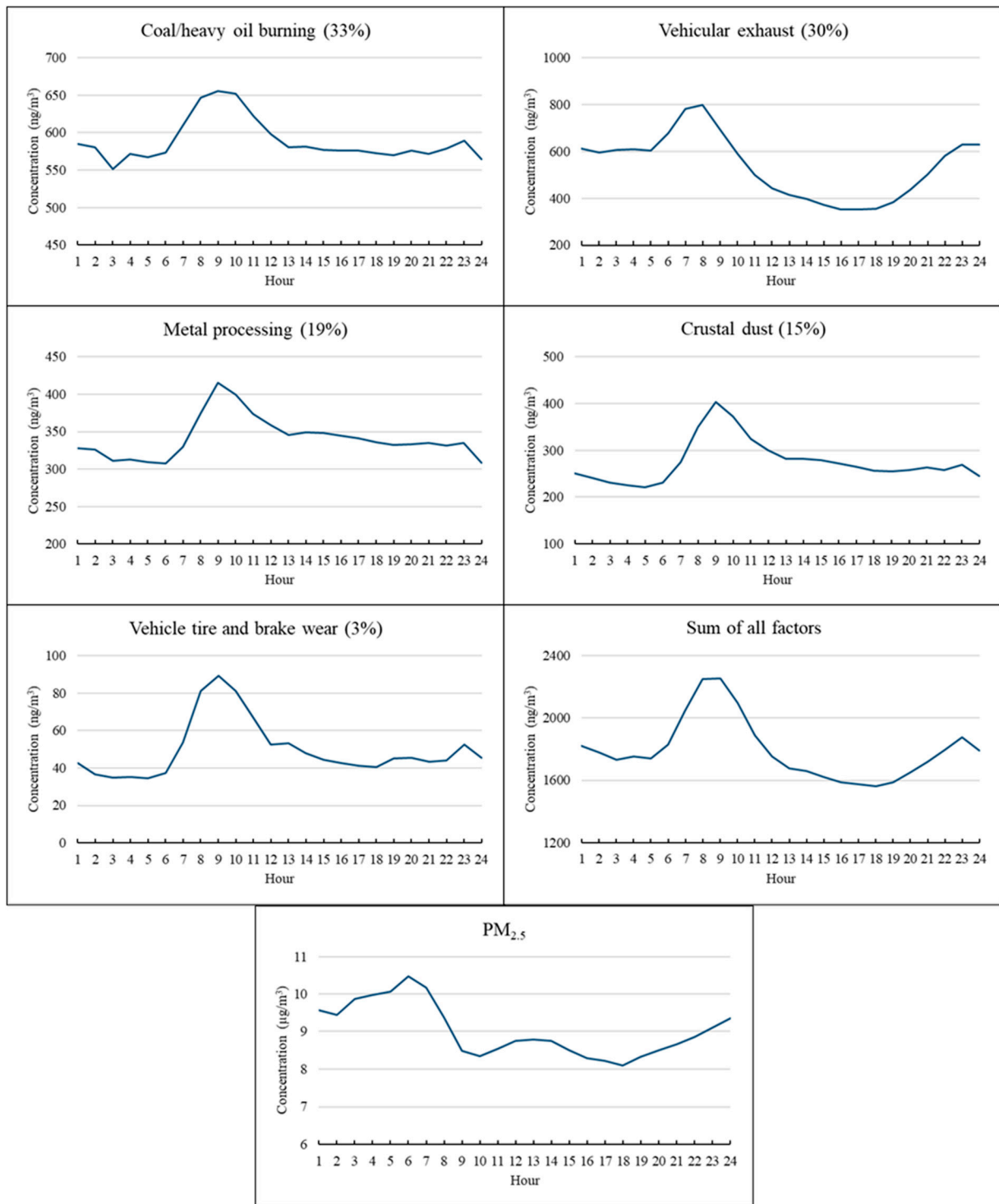


Figure S9. Diurnal variations of PMF estimated source contributions (ng/m^3) in Scenario 1 (percentages in the subtitles are average source contributions) and total concentrations of all factors, and observed PM_{2.5} concentration ($\mu\text{g/m}^3$).

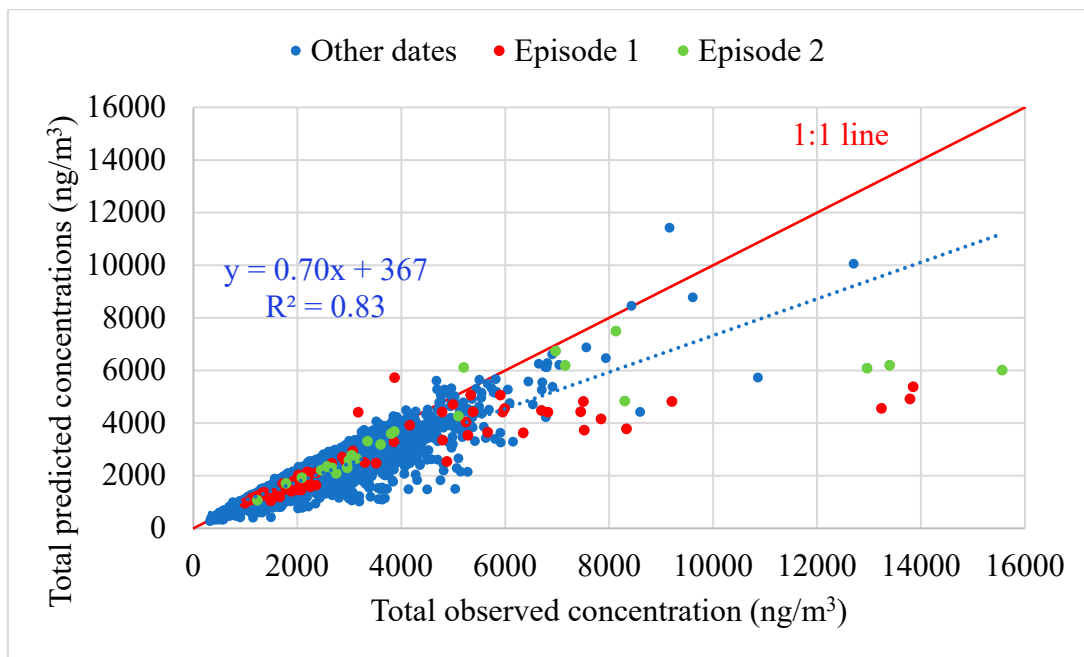


Figure S10. Scatter plot of hourly total observed vs. predicted concentrations (Scenario 1). The two episodes are labelled in red and green, respectively. When concentrations were greater than 4000 ng/m³, most of the hourly concentrations in the two episodes deviate further away from the 1:1 line.

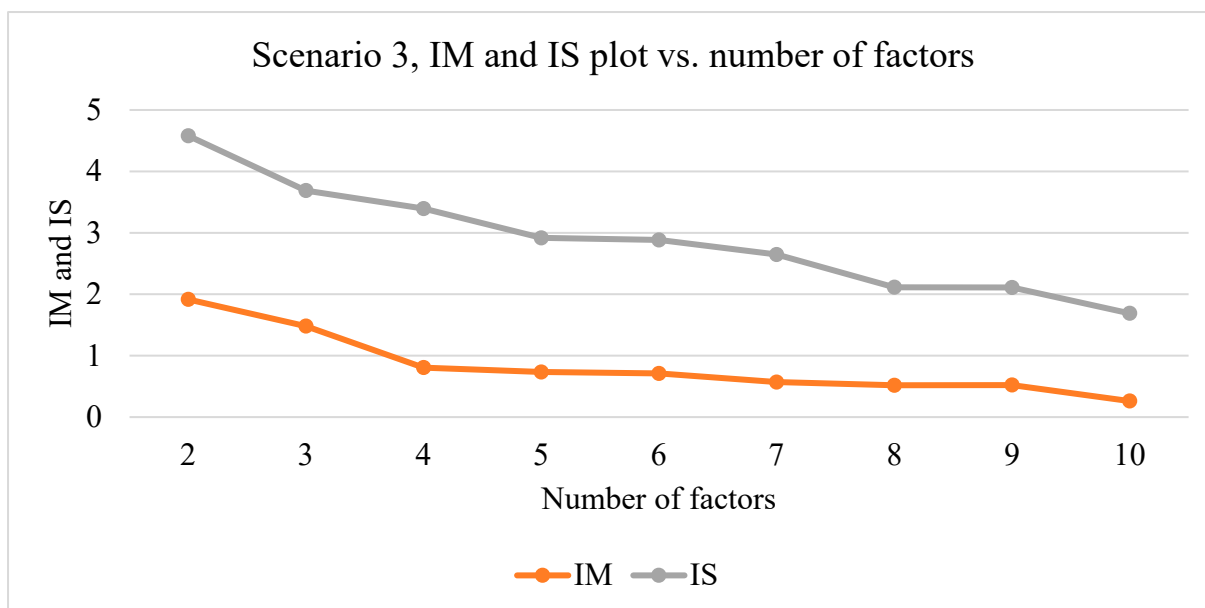


Figure S11. IM and IS vs. number of factors in Scenario 3.

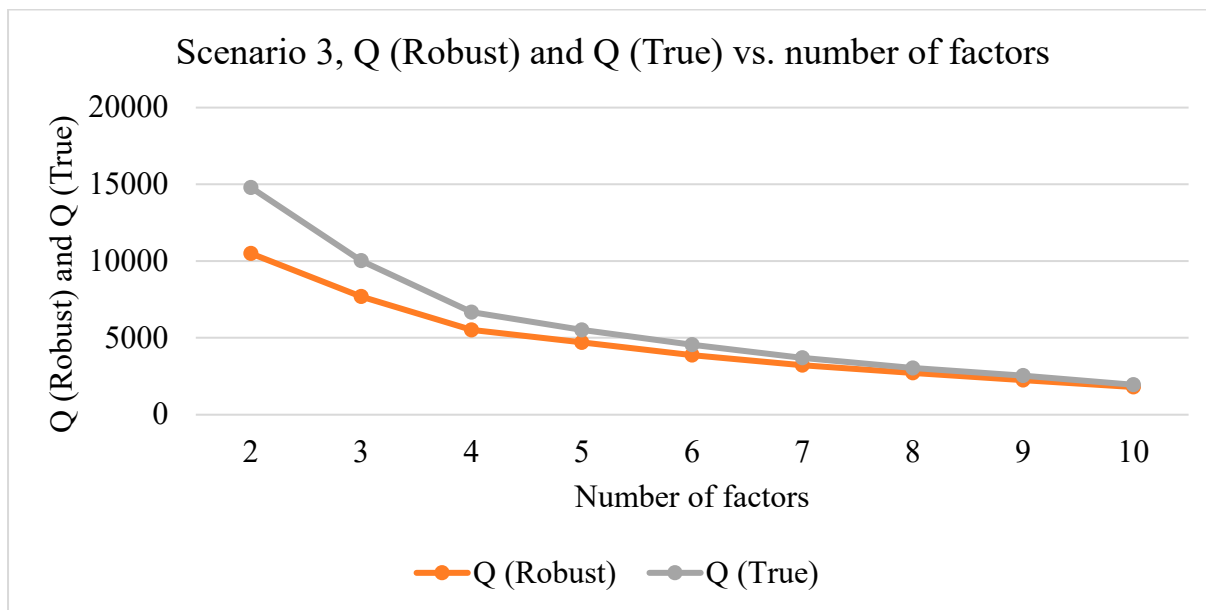


Figure S12. Q (Robust) and Q (True) vs. number of factors in Scenario 3.

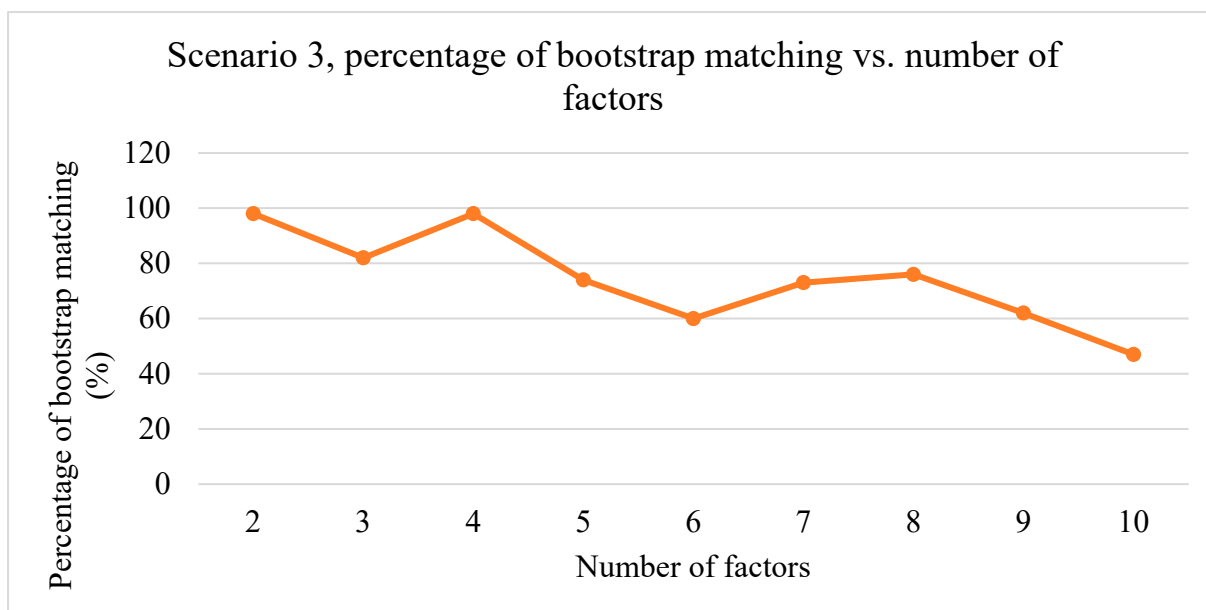


Figure S13. The percentage of bootstrap matching vs. number of factors in Scenario 3.

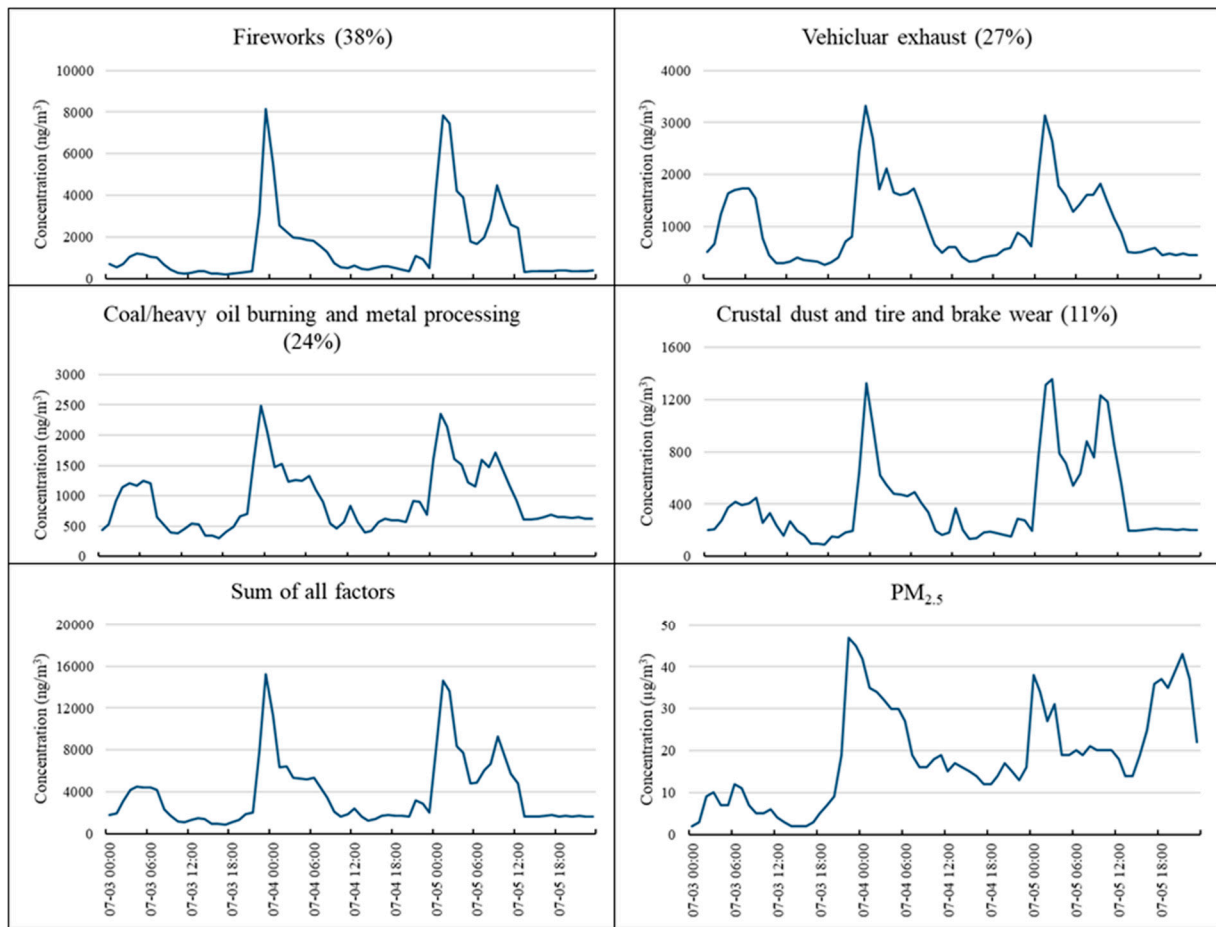


Figure S14. Time-series of PMF estimated factor concentrations (ng/m^3) in Scenario 3 (percentages in the subtitles are average source contributions) and total concentrations of all factors, and observed PM_{2.5} concentration ($\mu\text{g}/\text{m}^3$).

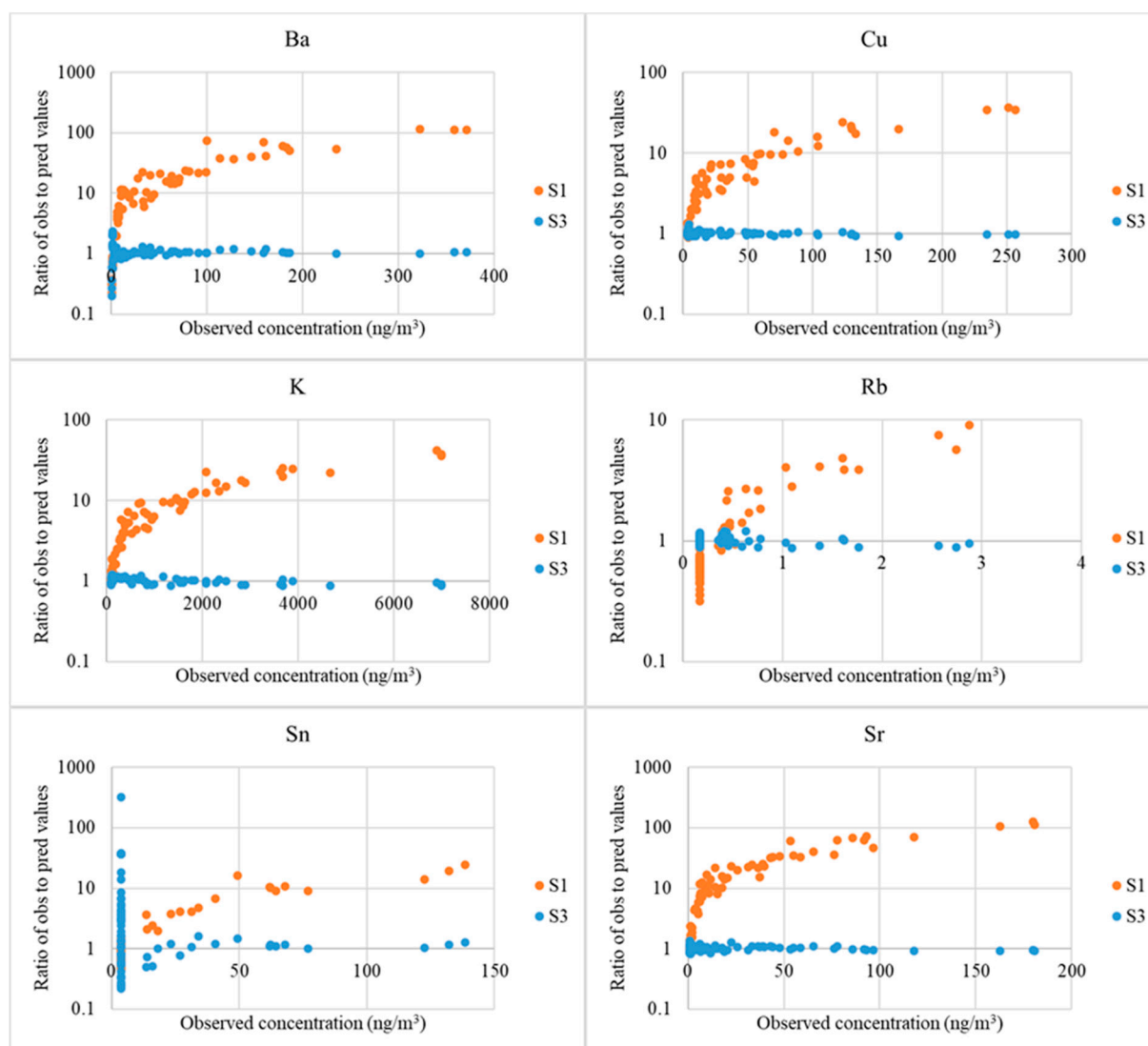


Figure S15. Ratios of observed to predicted concentrations for event markers in Scenarios 1 and 3 vs. observed concentrations.

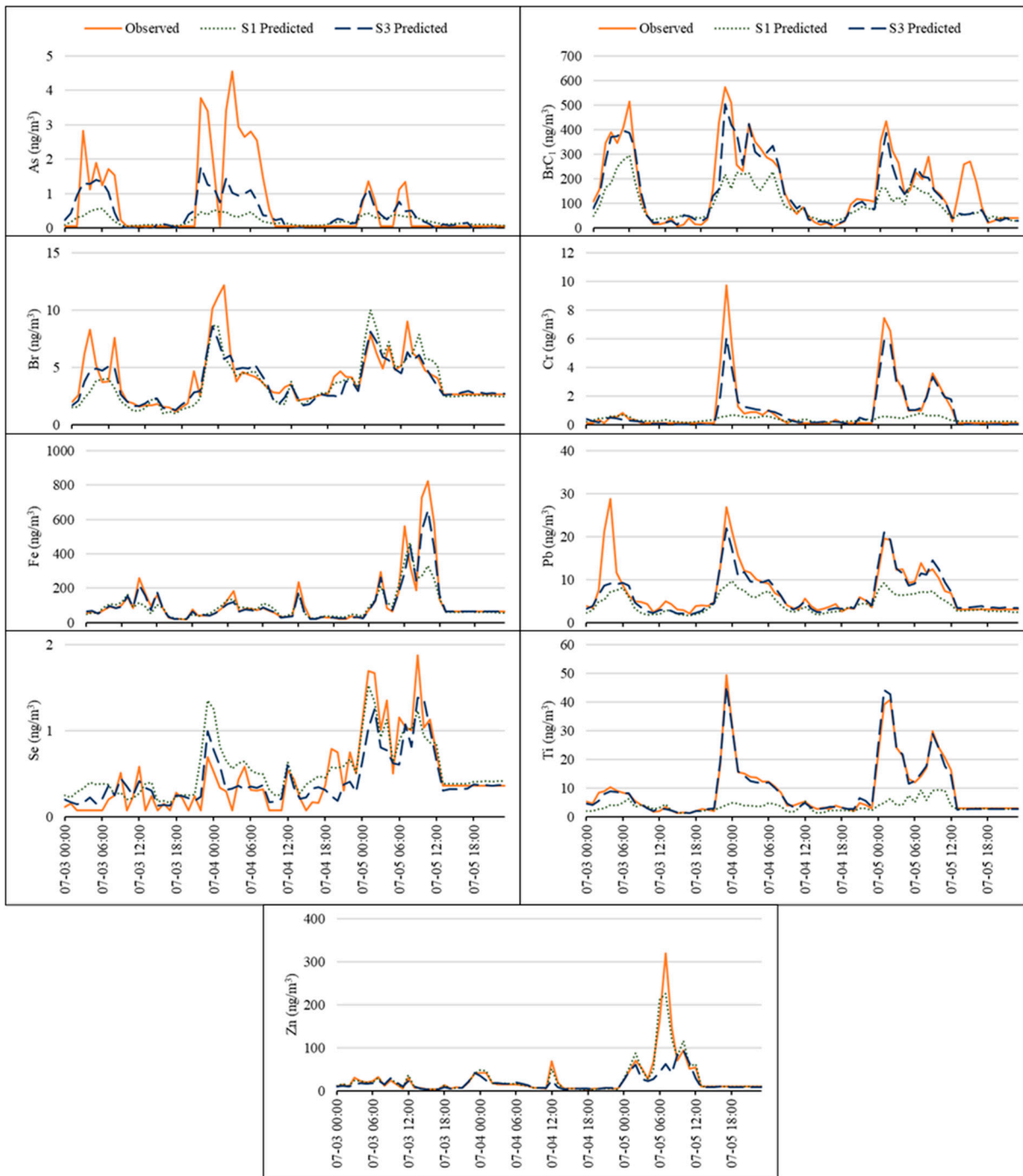


Figure S16. Time-series of hourly observed and predicted concentrations for As, BrC₁, Br, Cr, Fe, Pb, Se, Ti, and Zn during the episode on July 3-5, 2021 (Scenario 3). S1 and S3 in the figure legends correspond to Scenario 1 and Scenario 3, respectively.

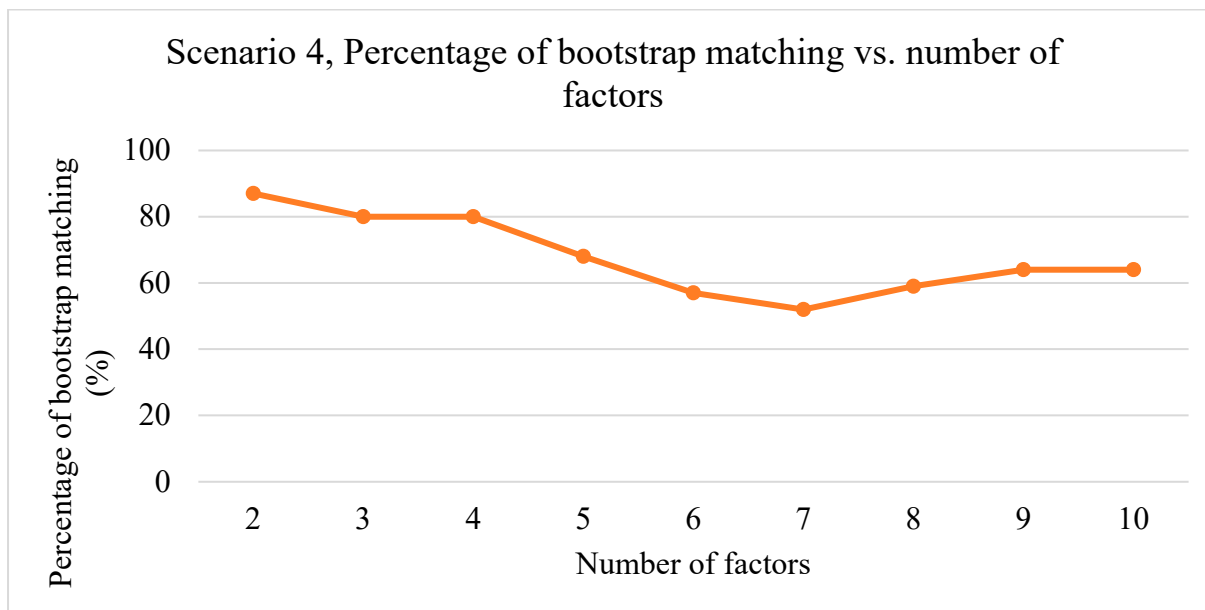


Figure S17. The percentage of bootstrap matching vs. number of factors in Scenario 4.

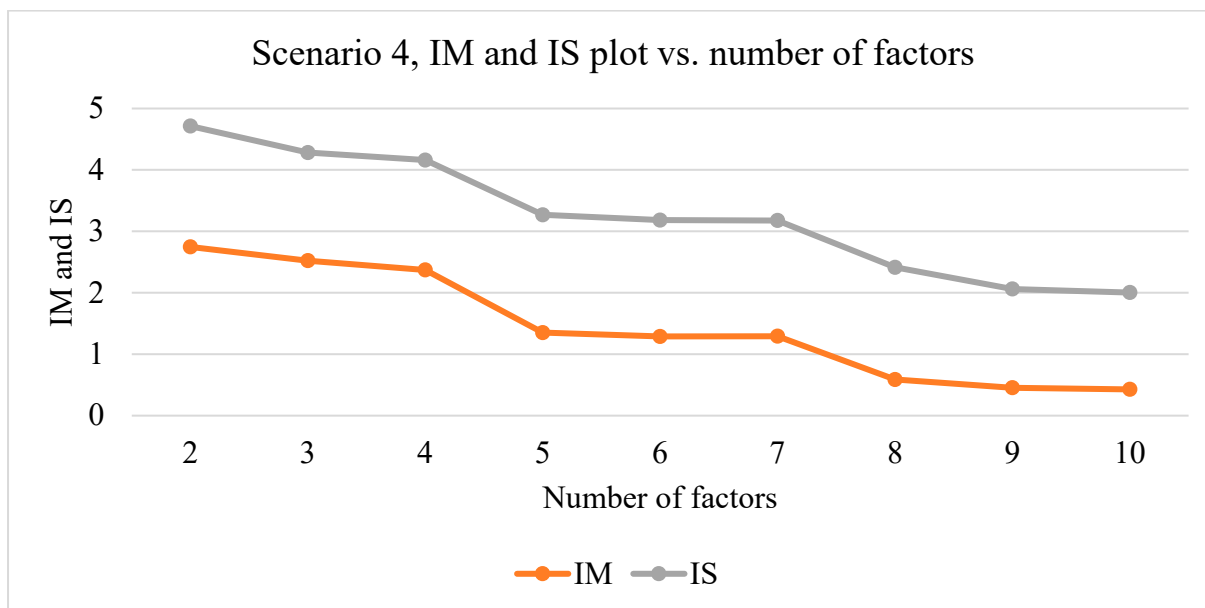


Figure S18. IM and IS vs. number of factors in Scenario 4.

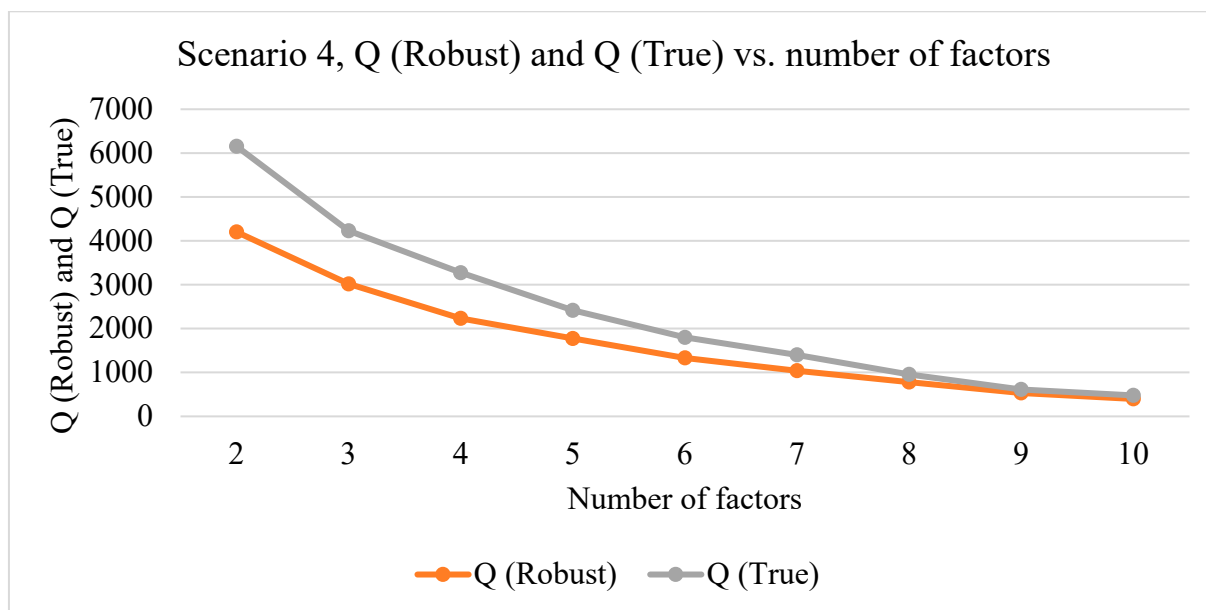


Figure S19. Q (Robust) and Q (True) vs. number of factors in Scenario 4.

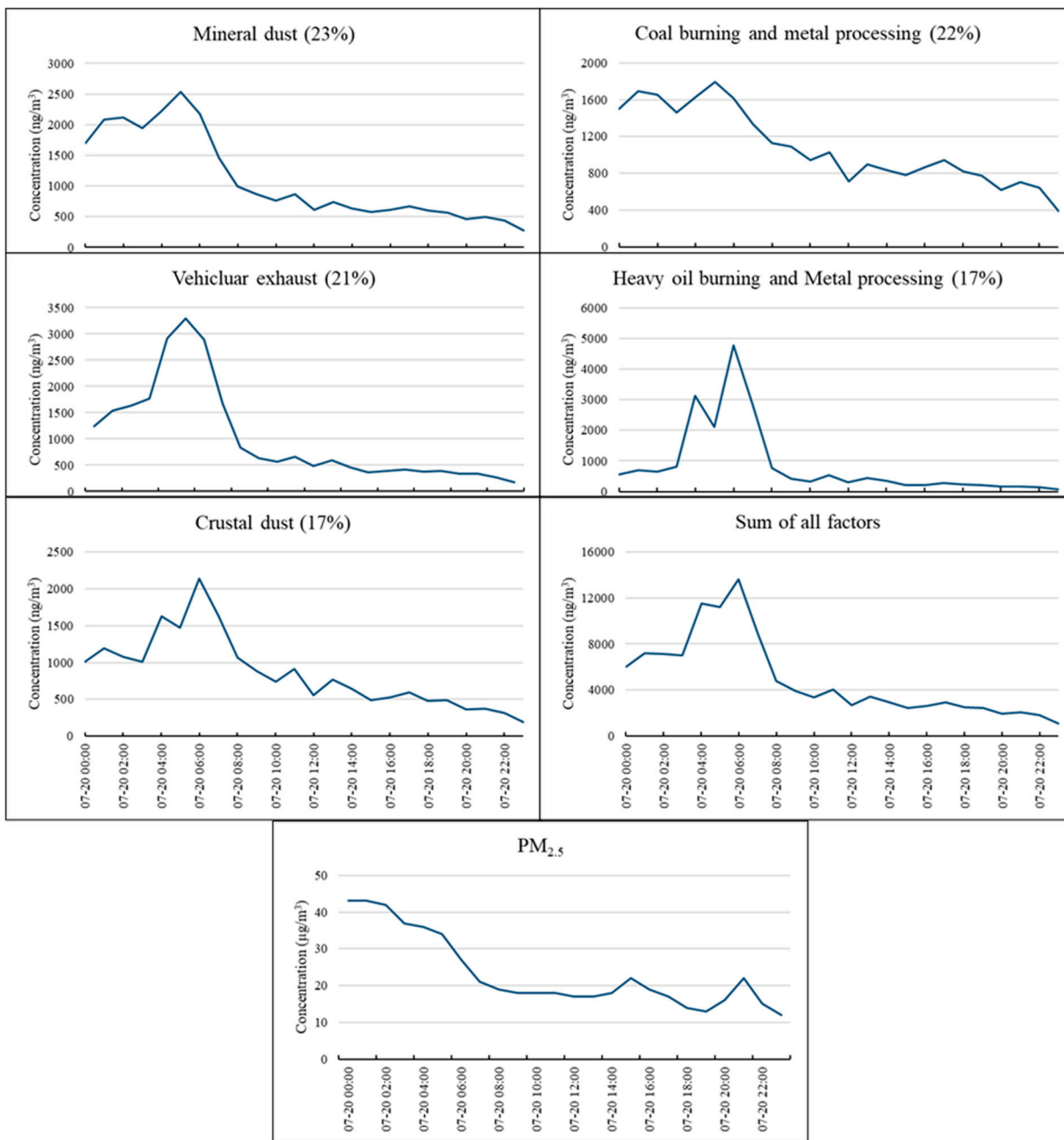


Figure S20. Time-series of PMF estimated factor concentrations (ng/m³) in Scenario 4 (percentages in the subtitles are average source contributions) and total concentrations of all factors, and observed PM_{2.5} concentration (µg/m³).

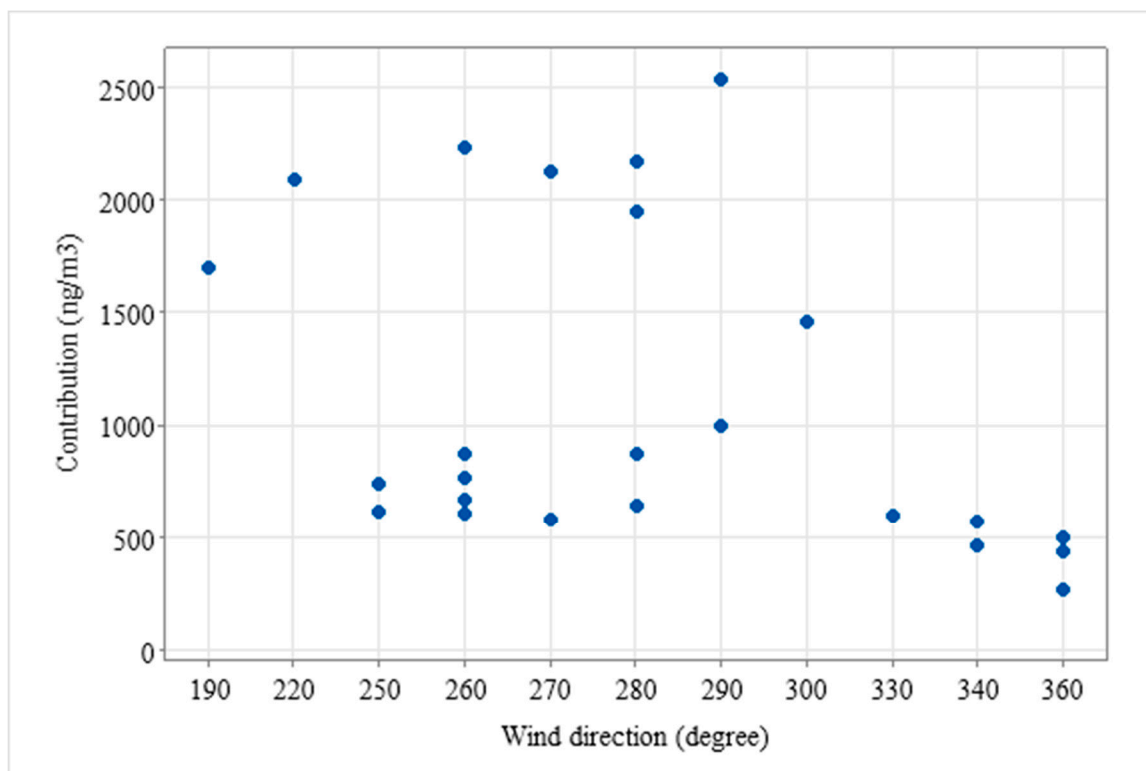


Figure S21. Source contributions of the mineral dust factor in Scenario 4 vs. hourly wind direction on July 20, 2021.

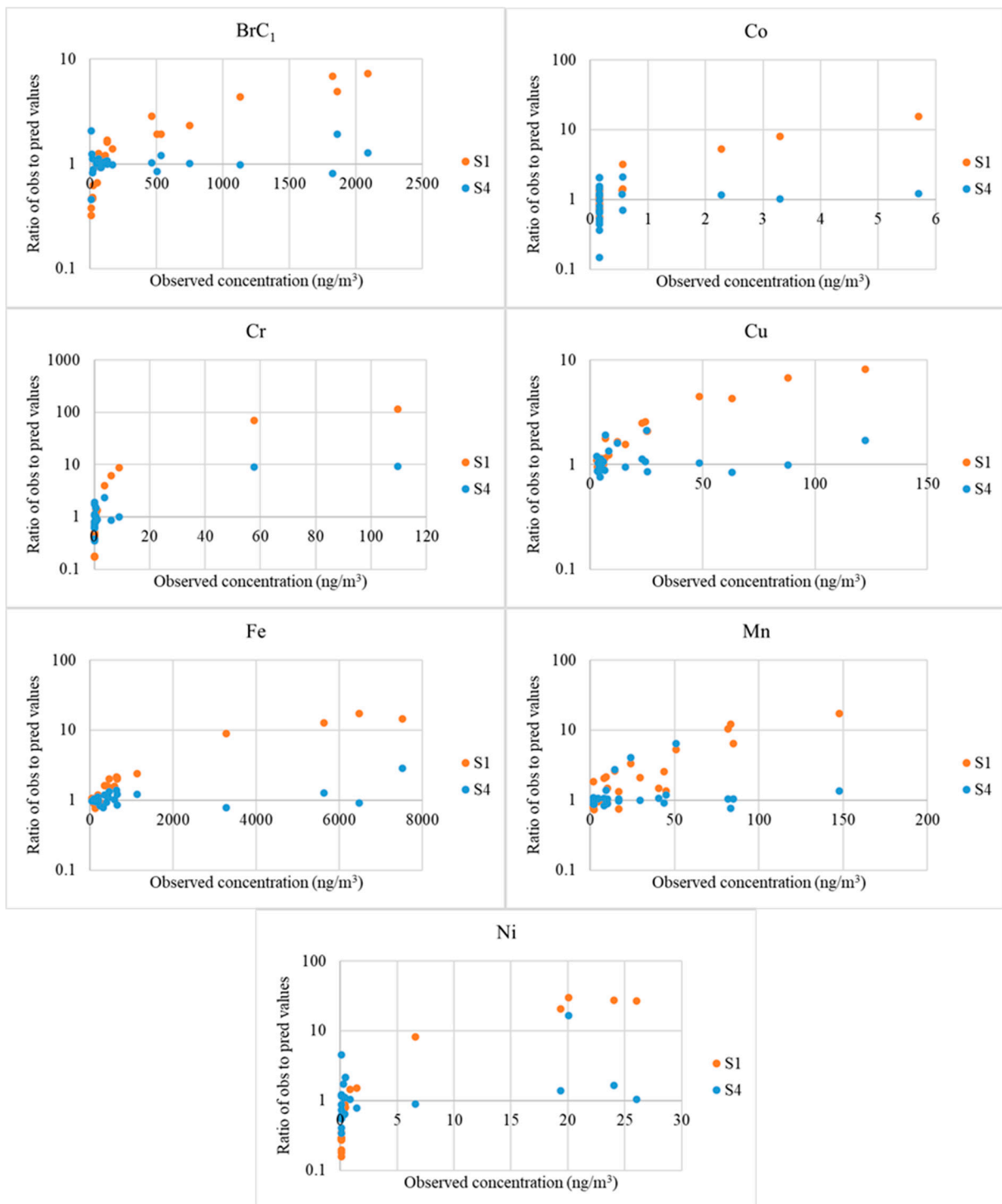


Figure S22. Ratios of observed to predicted concentrations for event markers in Scenarios 1 and 4 vs. observed concentrations.

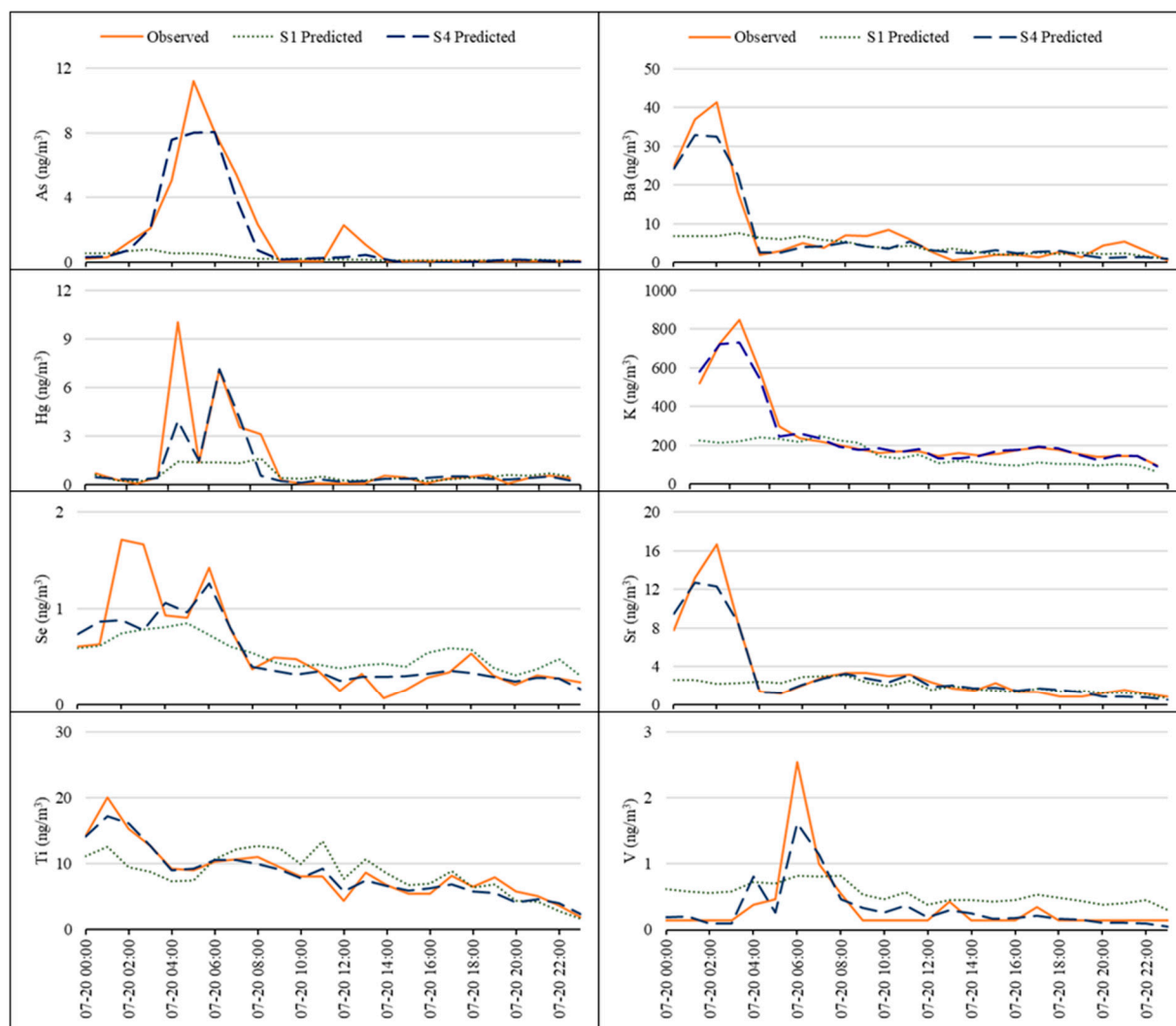


Figure S23. Time-series of hourly observed and predicted concentrations for As, Ba, Hg, K, Se, Sr, Ti and V during the episode of July 20, 2021 (Scenario 4). S1 and S4 in the figure legends correspond to Scenario 1 and Scenario 4, respectively.

References

- Zhang, T.; Su, Y.; Deboz, J.; Noble, M.; Munoz, A.; Xu, X. Continuous Measurements and Source Apportionment of Ambient PM_{2.5}-Bound Elements in Windsor, Canada. *Atmosphere* **2023**, *14*, 374. <https://doi.org/10.3390/atmos14020374>.
- Wang, H.; Zhang, L.; Cheng, I.; Yao, X.; Dabek-Zlotorzynska, E. Spatiotemporal trends of PM_{2.5} and its major chemical components at urban sites in Canada. *J. Environ. Sci.* **2021**, *103*, 1–11.
- Shin, S.M.; Kim, J.Y.; Lee, J.Y.; Kim, D.S.; Kim, Y.P. Enhancement of modeling performance by including organic markers to the PMF modeling for the PM_{2.5} at Seoul. *Air Qual. Atmos. Health* **2022**, *15*, 91–104.
- Chou, C.L. Sulfur in coals: A review of geochemistry and origins. *Int. J. Coal Geol.* **2012**, *100*, 1–13.
- Pekney, N.J.; Davidson, C.I.; Robinson, A.; Zhou, L.; Hopke, P.; Eatough, D.; Rogge, W.F. Major Source Categories for PM_{2.5} in Pittsburgh using PMF and UNMIX. *Aerosol Sci. Technol.* **2006**, *40*, 910–924.
- Wang, S.; Hu, G.; Yan, Y.; Wang, S.; Yu, R.; Cui, J. Source apportionment of metal elements in PM_{2.5} in a coastal city in Southeast China: Combined Pb-Sr-Nd isotopes with PMF method. *Atmos. Environ.* **2019**, *198*, 302–312.
- Hao, Y.; Meng, X.; Yu, X.; Lei, M.; Li, W.; Shi, F.; Xie, S. Characteristics of trace elements in PM_{2.5} and PM₁₀ of Chifeng, northeast China: Insights into spatiotemporal variations and sources. *Atmos. Res.* **2018**, *213*, 550–561.
- Chi, R.; Li, H.; Wang, Q.; Zhai, Q.; Wang, D.; Wu, M.; Liu, Q.; Wu, S.; Ma, Q.; Deng, F.; et al. Association of emergency room visits for respiratory diseases with sources of ambient PM_{2.5}. *J. Environ. Sci.* **2019**, *86*, 154–163.
- Sugiyama, T.; Shimada, K.; Miura, K.; Lin, N.-H.; Kim, Y.P.; Chan, C.K.; Takami, A.; Hatakeyama, S. Measurement of ambient PAHs in Kumamoto: Differentiating local and transboundary air pollution. *Aerosol Air Qual. Res.* **2017**, *17*, 3106–3118.
- Ontario Environment and Energy (OEE). The End of Coal. 2021. Available online: <https://www.ontario.ca/page/end-coal> (accessed on 20 May 2023).

11. United States Energy Information Administration (USEIA). Michigan State Energy Profile. 2022. Available online: <https://www.eia.gov/state/print.php?sid=MI#:~:text=Michigan%20Quick%20Facts&text=In%202021%2C%20coal%20provided%20the,three%2Dfifths%20of%20that%20power> (accessed on 20 May 2023).
12. Sofowote, U.M.; Su, Y.; Dabek-Zlotorzynska, E.; Rastogi, A.K.; Brook, J.; Hopke, P.K. Sources and temporal variations of constrained PMF factors obtained from multiple-year receptor modeling of ambient PM_{2.5} data from five speciation sites in Ontario, Canada. *Atmos. Environ.* **2015**, *108*, 140–150.
13. Choi, S.; Park, J.-H.; Kim, W.; Kim, S.W.; Lee, K.-H.; Chung, T.; Park, J.; Ryu, S.-H.; Shin, J.; Koh, D.-H.; et al. Black Carbon Exposure Characteristics in Diesel Engine Vehicle-related Jobs. *Aerosol Air Qual. Res.* **2021**, *21*, 200675.
14. Chen, R.; Zhao, Y.; Tian, Y.; Feng, X.; Feng, Y. Sources and uncertainties of health risks for PM_{2.5}-bound heavy metals based on synchronous online and offline filter-based measurements in a Chinese megacity. *Environ. Int.* **2022**, *164*, 107236.
15. Landis, M.S.; Lewis, C.W.; Stevens, R.K.; Keeler, G.J.; Dvonch, J.T.; Tremblay, R.T. Ft. McHenry tunnel study: Source profiles and mercury emissions from diesel and gasoline powered vehicles. *Atmos. Environ.* **2007**, *41*, 8711–8724.
16. Balakrishna, G.; Pervez, S.; Bisht, D.S. Source apportionment of arsenic in atmospheric dust fall out in an urban residential area, Raipur, Central India. *Atmos. Chem. Phys.* **2011**, *11*, 5141–5151.
17. Hsu, C. Y., Chiang, H. C., Chen, M. J., Chuang, C. Y., Tsen, C. M., Fang, G. C., ... & Chen, Y. C. Ambient PM_{2.5} in the residential area near industrial complexes: Spatiotemporal variation, source apportionment, and health impact. *Sci. Total Environ.* **2017**, *590*, 204–214.
18. Wang, J.; Jiang, H.; Jiang, H.; Mo, Y.; Geng, X.; Li, J.; Mao, S.; Bualert, S.; Ma, S.; Li, J.; et al. Source apportionment of water-soluble oxidative potential in ambient total suspended particulate from Bangkok: Biomass burning versus fossil fuel combustion. *Atmos. Environ.* **2020**, *235*, 117624.
19. Yu, Y.; He, S.; Wu, X.; Zhang, C.; Yao, Y.; Liao, H.; Wang, Q.; Xie, M. PM_{2.5} elements at an urban site in Yangtze River Delta, China: High time-resolved measurement and the application in source apportionment. *Environ. Pollut.* **2019**, *253*, 1089–1099.
20. Harrison, R.M.; Jones, A.M.; Gietl, J.; Yin, J.; Green, D.C. Estimation of the contributions of brake dust, tire wear, and resuspension to nonexhaust traffic particles derived from atmospheric measurements. *Environ. Sci. Technol.* **2012**, *46*, 6523–6529.
21. Farahani, V.J.; Soleimani, E.; Pirhadi, M.; Sioutas, C. Long-term trends in concentrations and sources of PM_{2.5}-bound metals and elements in central Los Angeles. *Atmos. Environ.* **2021**, *253*, 118361.
22. Taghvaei, S.; Sowlat, M.H.; Mousavi, A.; Hassanvand, M.S.; Yunesian, M.; Naddafi, K.; Sioutas, C. Source apportionment of ambient PM_{2.5} in two locations in central Tehran using the Positive Matrix Factorization (PMF) model. *Sci. Total Environ.* **2018**, *628*, 672–686.
23. Oliver, J. Fireworks Near Me: Detroit's 4th of July 2021. Available online: <https://patch.com/michigan/detroit/fireworks-near-me-detroits-4th-july-2021> (accessed on 20 May 2023).
24. Michigan Live. July 4 Fireworks, Festivals and Other Events in Michigan. 2021. Available online: <https://www.mlive.com/news/2021/06/july-4-fireworks-festivals-and-other-events-in-michigan.html> (accessed on 20 May 2023).